

Fig. S1

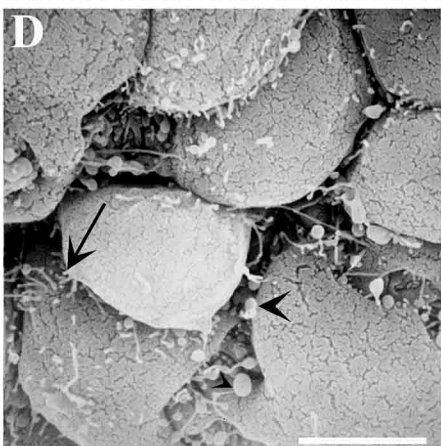
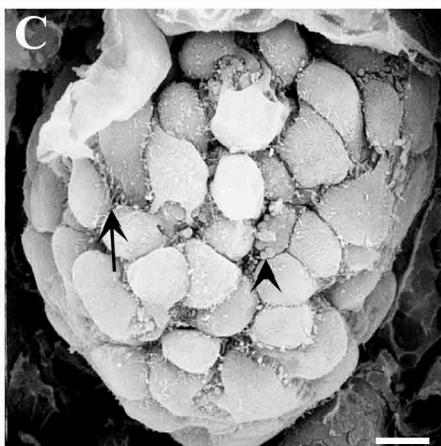
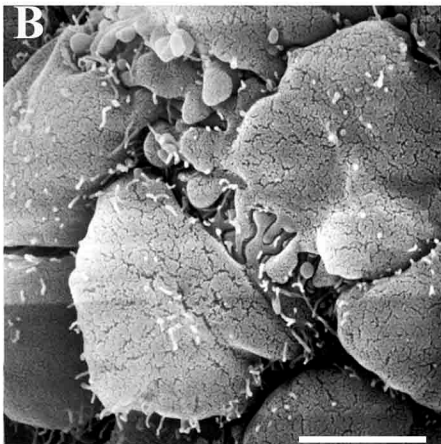
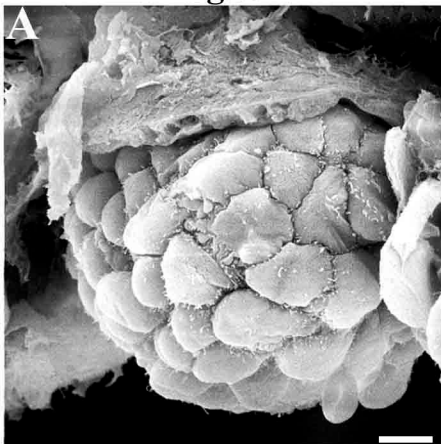
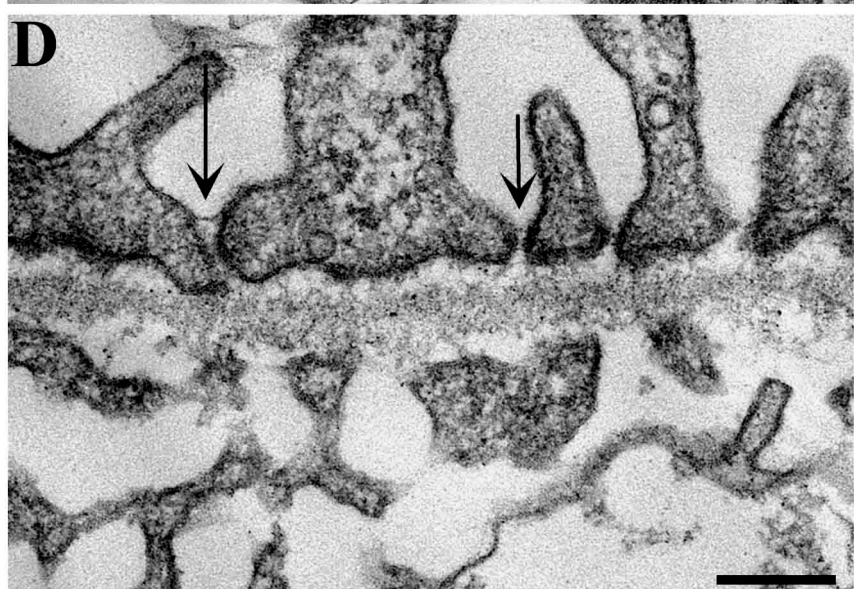
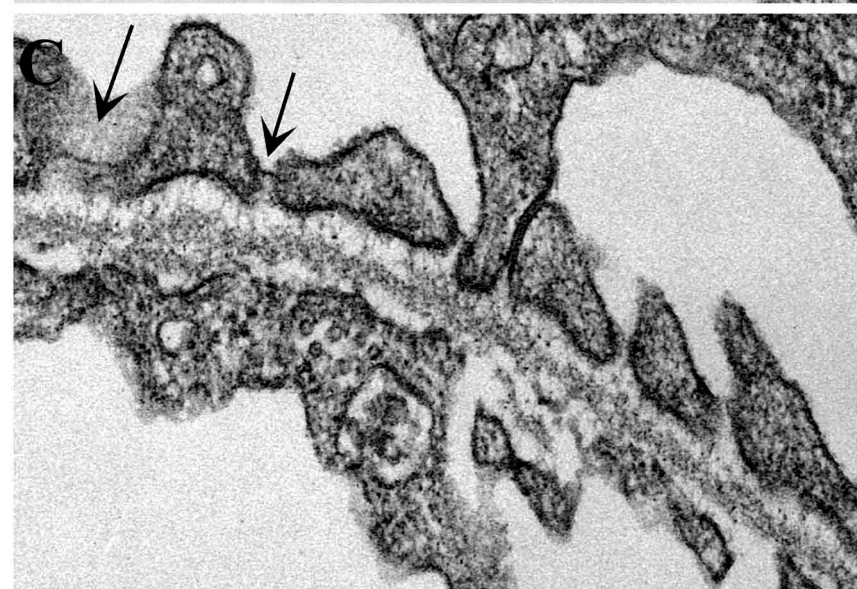
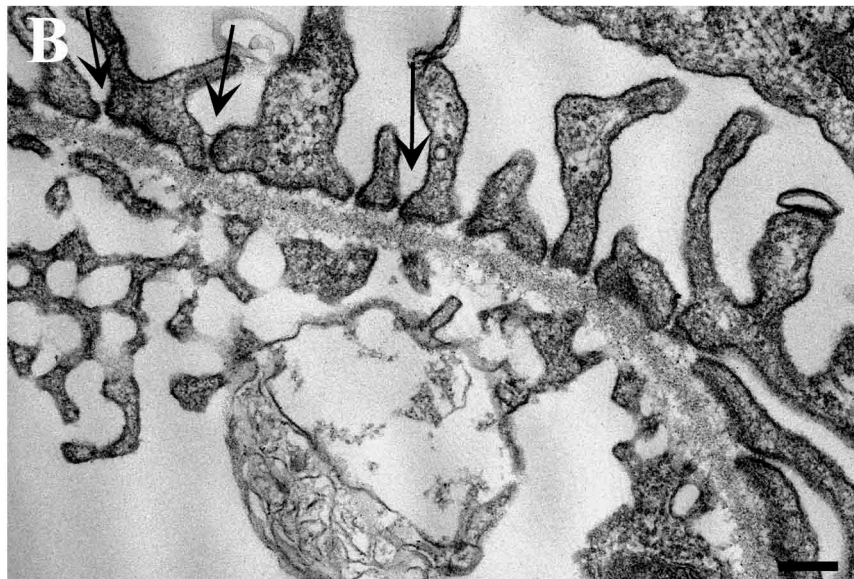
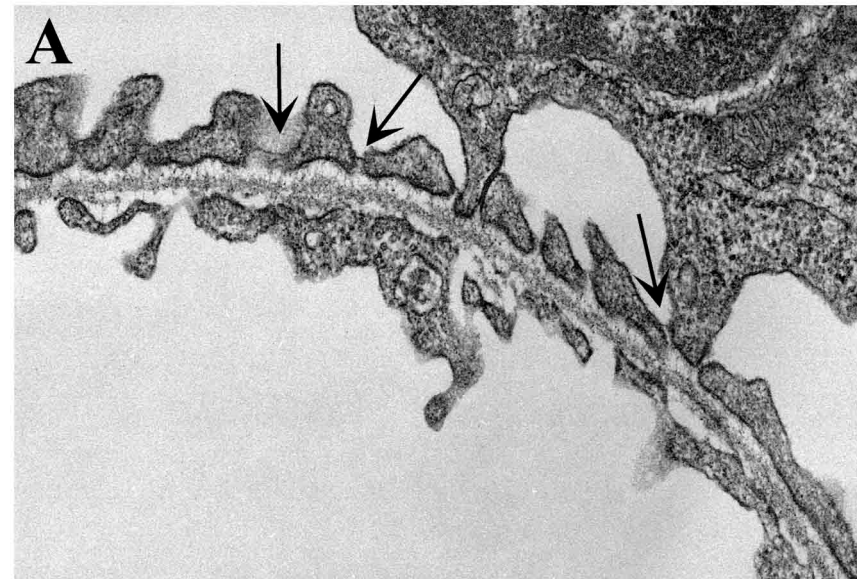


Figure S2



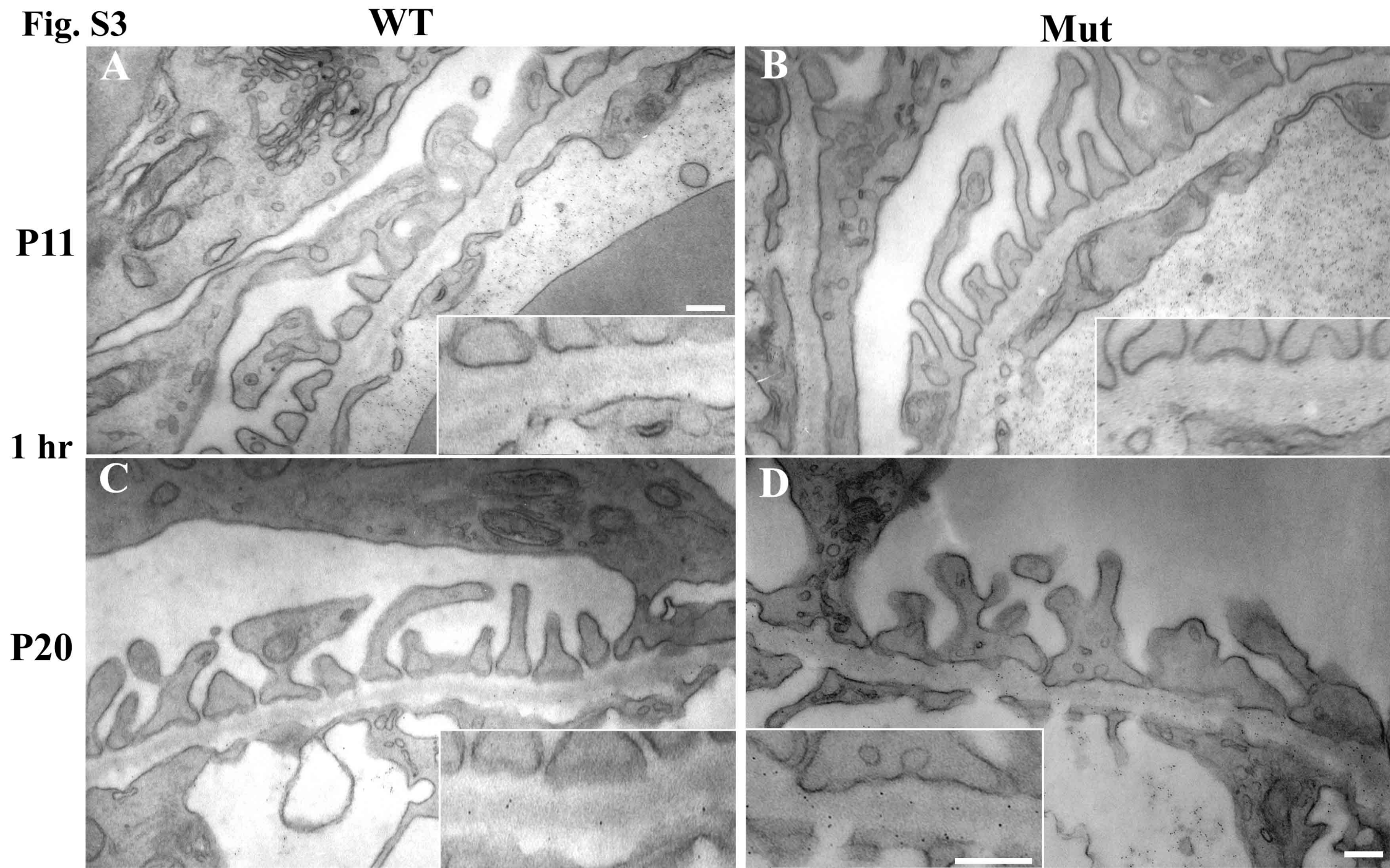


Fig. S4

WT

Mut

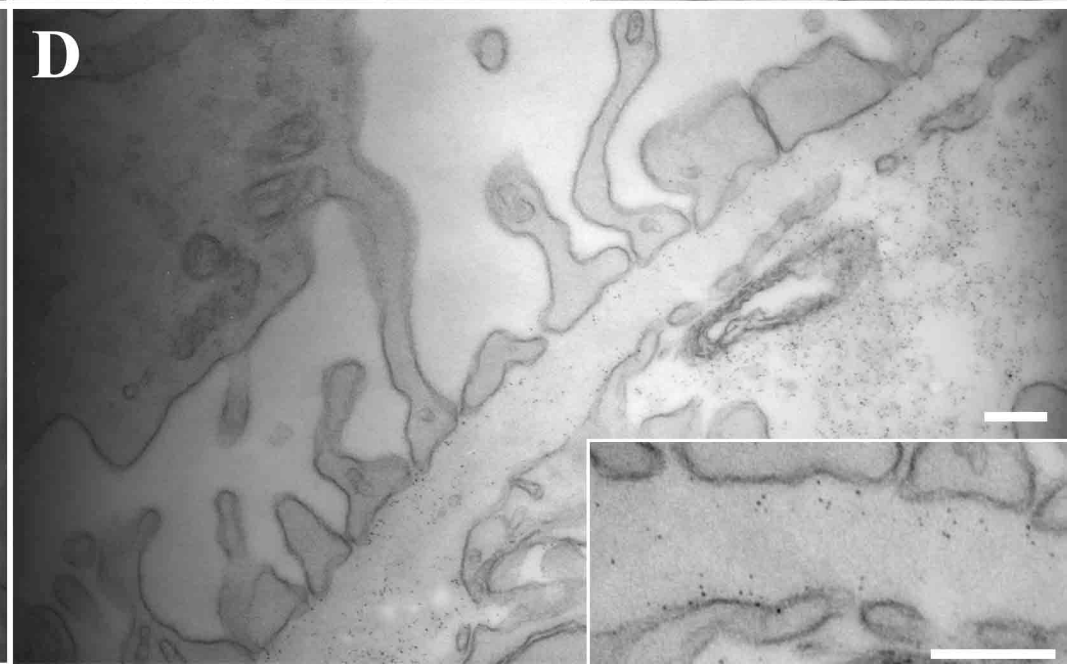
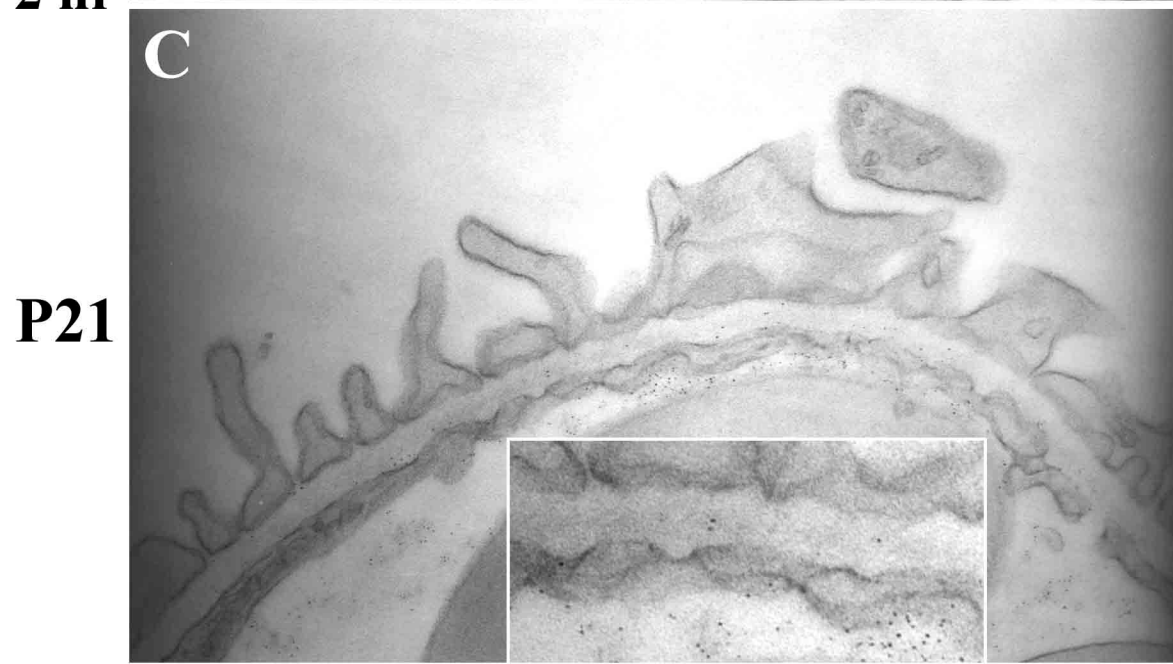
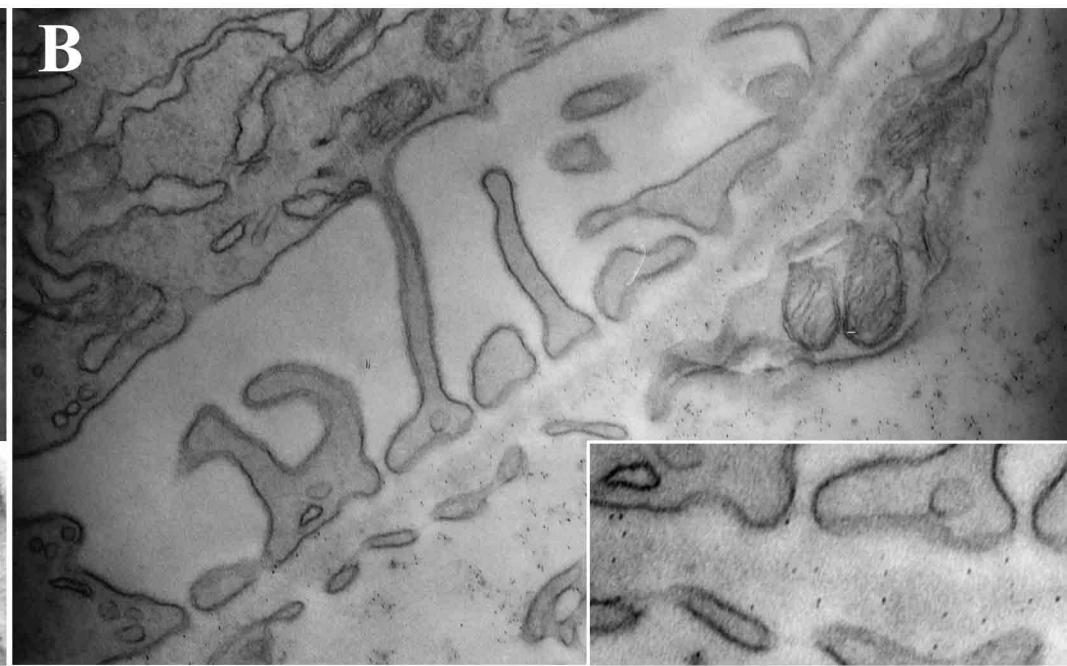
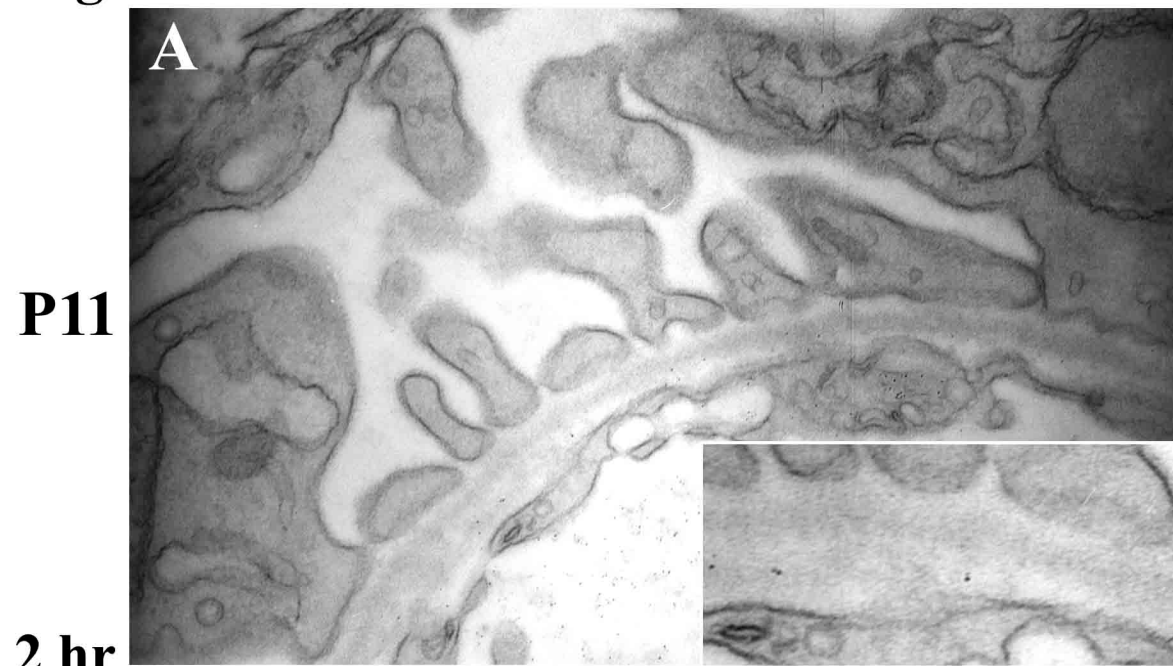


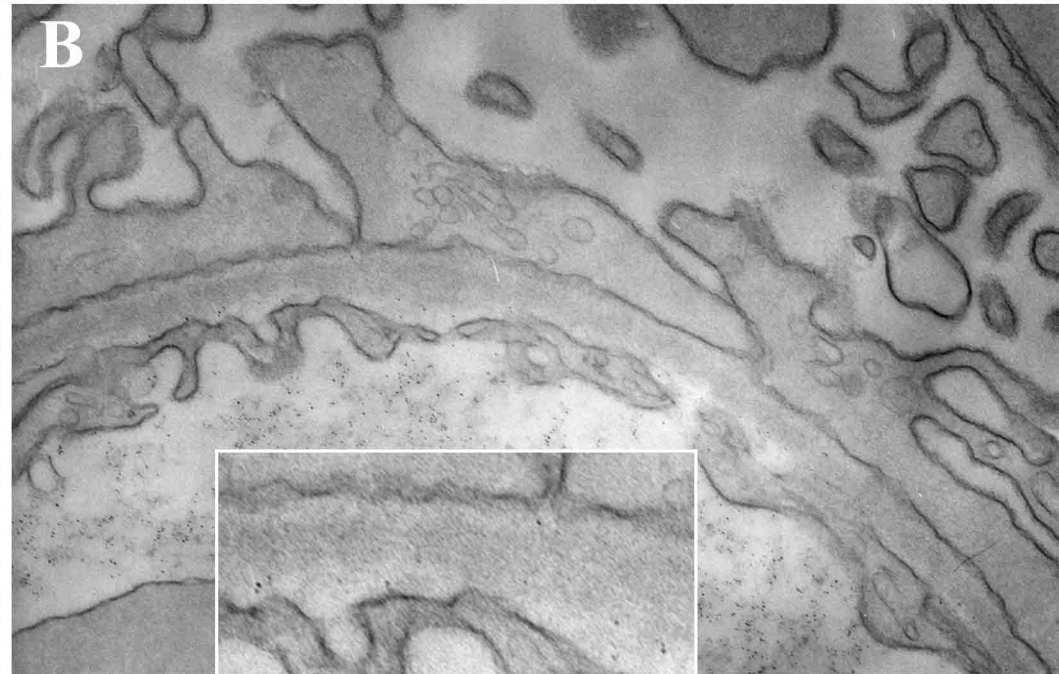
Fig. S5

WT

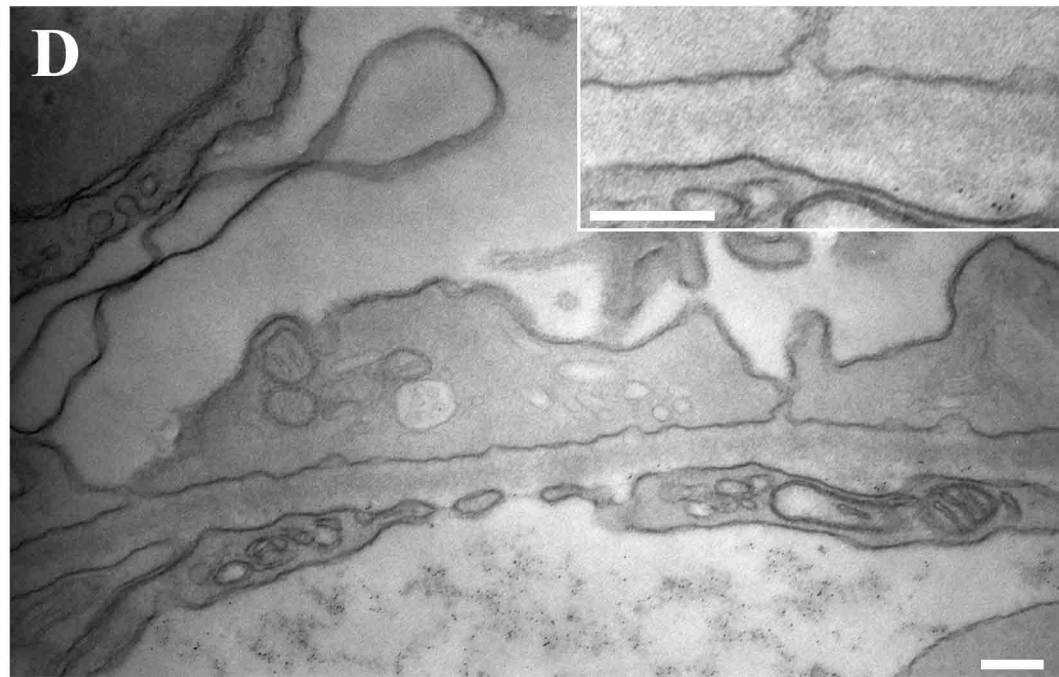
P 21

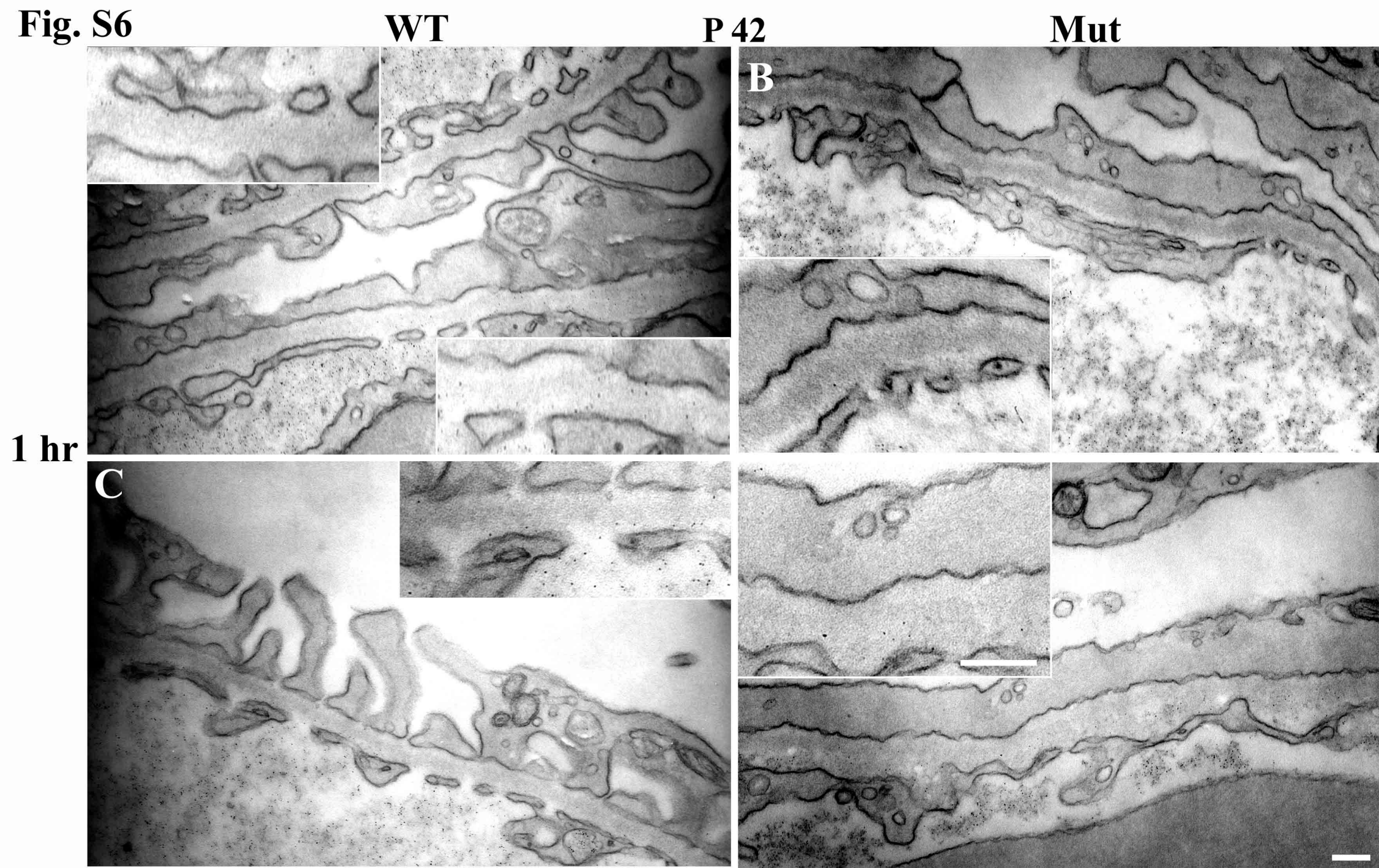
Mut

1 hr



2 hr





Supplemental Figure Legends

Figure S1. SEM shows extensive villous transformation of *Lamb2*^{-/-} podocytes.

Glomeruli from P5 mice were visualized using SEM at two magnifications. (A, B) An immature control glomerulus before the appearance of foot processes and before podocyte cell body maturation. (C, D) An immature *Lamb2*^{-/-} glomerulus exhibits mild changes to the apical surface of podocytes in the form of villous transformation (arrow in C) and blebbing (arrowheads in C, D). Bars = 5 μ m.

Figure S2. TEM shows normal foot process and SD architecture in the absence of β 2 at P5.

TEM micrographs of mature P5 glomeruli from control (A, C) and proteinuric *Lamb2*^{-/-} (B, D) mice. Note the presence of SDs (arrows) and normal FP architecture in both. C and D are higher magnification of A and B, respectively. Bars = 200 nm.

Figure S3. *Lamb2*^{-/-} GBM ferritin permeability after 1 hour.

Ferritin was injected intravenously into control (A, C) and *Lamb2*^{-/-} (B, D) mice at P11 (A, B) or P20 (C, D), and kidneys were fixed in situ 1 hr after injection and processed for TEM. There was an increase in the number of ferritin particles throughout the GBM at both ages, even in areas of intact foot processes. This increase was most obvious in the subepithelial aspect of the GBM, corresponding to the LRE. Note the higher magnification insets. Bar = 125 nm.

Figure S4. *Lamb2*^{-/-} GBM ferritin permeability after 2 hours.

Ferritin was injected intravenously into control (A, C) and *Lamb2*^{-/-} (B, D) mice at P11 (A, B) or P21 (C, D), and kidneys were fixed in situ 2 hrs after injection and processed for TEM. There was an increase in the number of ferritin particles throughout the GBM at both ages, even in areas of intact foot processes. This increase was most obvious in the subepithelial aspect of the GBM, corresponding to the LRE. Note the higher magnification insets. Bar = 125 nm.

Figure S5. GBM ferritin permeability in P21 *Cd2ap*^{-/-} mice.

Control (A, C) or nephrotic *Cd2ap*^{-/-} (B, D) mice were injected with ferritin. Kidneys were fixed in situ after either 1 (A, B) or 2 hours (C, D). TEM showed normal ferritin distribution in the GBM even in areas of foot process effacement. Note the higher magnification insets. Bar = 125 nm.

Figure S6. GBM ferritin permeability in 6 week old *Cd2ap*^{-/-} mice.

Control (A, C) or nephrotic *Cd2ap*^{-/-} (B, D) mice were injected with ferritin. Kidneys were fixed in situ after 1 hr. TEM showed that despite widespread foot processes effacement, GBM ferritin distribution in the mutant was comparable to control. Note the higher magnification insets. Bar = 125 nm.